

Molecular gas and the dynamics of galaxies

F. Combes

*Observatoire de Paris, DEMIRM, 61 Av. de l'Observatoire, F-75014,
Paris, France*

Abstract. In this review, I discuss some highlights of recent research on molecular gas in galaxies; large-scale CO maps of nearby galaxies are being made, which extend our knowledge on global properties, radial gradients, and spiral structure of the molecular ISM. Very high resolution are provided by the interferometers, that reveal high velocity gradients in galaxy nuclei, and formation of embedded structures, like bars within bars. Observation of the CO and other lines in starburst galaxies have questioned the H₂-to-CO conversion factor. Surveys of dwarfs have shown how the conversion factor depends on metallicity. The molecular content is not deficient in galaxy clusters, as is the atomic gas. Galaxy interactions are very effective to enhance gas concentrations and trigger starbursts. Nuclear disks or rings are frequently observed, that concentrate the star formation activity. Since the density of starbursting galaxies is strongly increasing with redshift, the CO lines are a privileged tool to follow evolution of galaxies and observe the ISM dynamics at high redshift: due to the high excitation of the molecular gas, the stronger high- J CO lines are redshifted into the observable band, which facilitates the detection.

In the last years, progress has been very rapid in the domain of molecules at high redshift, and we now know in better detail the molecular content in several systems beyond $z = 1$ and up to $z \sim 5$, either through millimeter and sub-millimeter emission lines, continuum dust emission, or millimeter absorption lines in front of quasars. More and more systems are gravitationally lensed, which helps the detection, but also complicates the interpretation. The detection of all these systems could give an answer about the debated question of the star-formation rate as a function of redshift. The maximum of star-formation rate, found around $z = 2$ from optical studies, could shift to higher z if the most remote objects are hidden by dust.

1. CO and H₂ content of galaxies

Although the molecular component is a key parameter for the star formation history and the evolution of galaxy disks, their H₂ content is still very uncertain, mainly because the bulk of the gas is not seen directly, but through questionable tracers, such as the CO lines. The wider surveys now available, together with the observations of starbursts and the more sensitive observations of low metallicity galaxies now have revealed how variable can be the CO to H₂ conversion ratio,

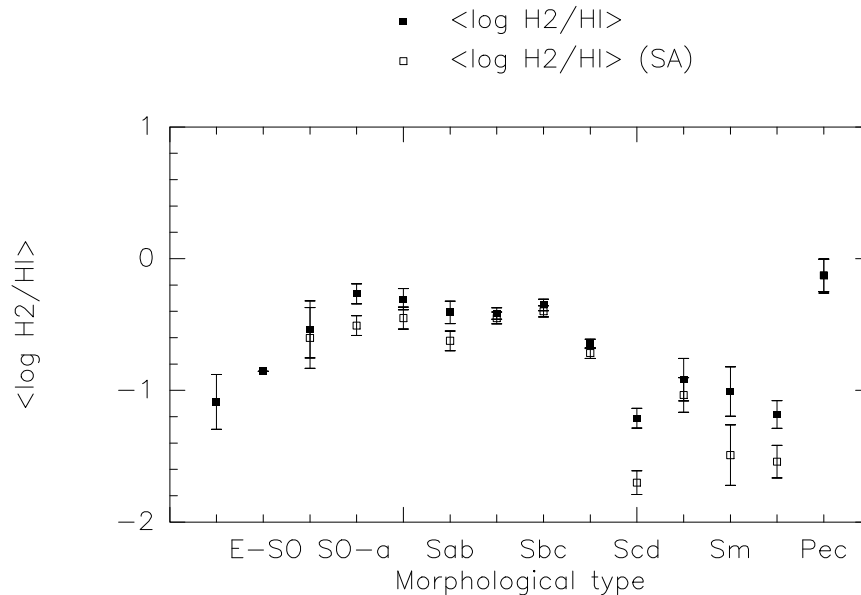


Figure 1. H_2/HI mass ratio in galaxies as a function of morphological type; full squares: mean values with upper limits treated as detections; empty squares: mean values with upper limits taken into account using the survival analysis (SA), from Casoli et al (1998).

that was previously thought constant within $\pm 50\%$ (Young & Scoville 1991). Also, the first surveys were oriented towards star forming galaxies, selected from far-infrared (IRAS) samples, and those happened to be rich CO emitters (according to the well established FIR-CO correlation). When more galaxies are included, the derived H_2/HI mass ratio in galaxies becomes lower than 1, the previously established value, to be around 0.2 in average (Casoli et al 1998).

The dependence of the molecular content with type also has been refined; the apparent H_2/HI mass ratio decreases monotonously from SO to Sm galaxies, but the extremes were separated by a factor 20-30 (Young & Knezek 1989), which is now reduced to about 10 (cf fig.1, Casoli et al 1998). This gradient towards the late-types might be only due to a reduced CO emission, because of metallicity effects, and not to an intrinsic reduction of the H_2 content. When only the more massive objects are taken into account, this tendency with type does not appear: there is no gradient of molecular fraction. This supports the hypothesis that the gradient is due to metallicity, which is correlated with total mass.

The dependence of the CO-to- H_2 conversion factor X with metallicity has been confirmed now in many galaxies. In the Small Magellanic Clouds, X could be 10 times higher than the standard value of $2.3 \cdot 10^{20} \text{ mol cm}^{-2} (\text{K.km/s})^{-1}$ (Rubio et al 1993). The effect has been seen also in local group galaxies, such as M31, M33, NGC 6822 and IC10 (Wilson 1995). The physical explanation is complex, since the CO lines are optically thick, but the size of the clouds

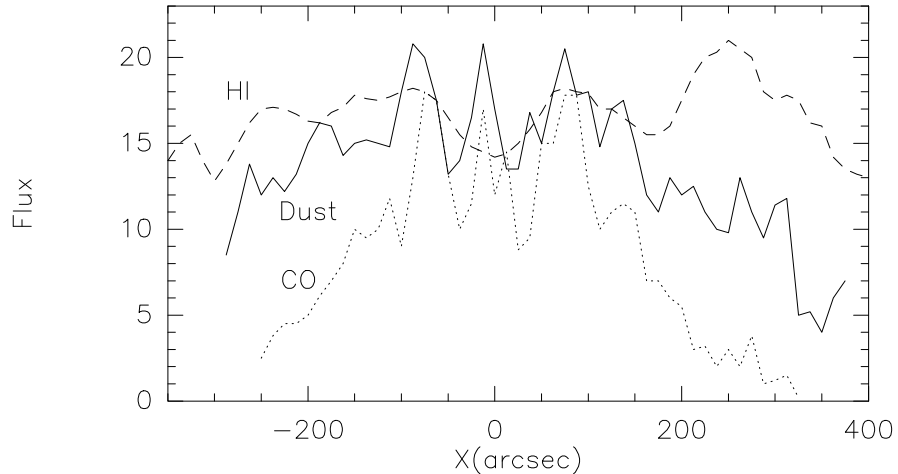


Figure 2. Dust emission radial profile in NGC 4565, compared to the CO and HI profiles, from Neininger et al (1996).

(and therefore the filling factor) decreases with metallicity, both due to direct CO abundance, and UV-photodissociation increased by the depletion of dust. When the dust is depleted by a factor 20, there is only 10% less H_2 but 95% less CO (Maloney & Black 1988).

Another tracer of the molecular gas has been widely used in recent years: cold dust emission, through galaxy mapping with bolometers at 1.3mm. The technique is best suited to edge-on galaxies, since a nearby empty reference position must be frequently observed to eliminate atmospheric gradients. One of the first observed, NGC 891, has a radial dust emission profile exactly superposable to the CO-emission profile (Guelin et al 1993). At 3mm, the dust is completely optically thin, and therefore the emission is proportional to the dust abundance, or the metallicity Z . The identity between the dust and CO emission profiles tend to confirm the strong dependence of CO emission with Z . In some galaxies, the CO emission falls off radially even faster than the dust emission; it is the case of NGC 4565 or NGC 5907 for example (cf fig 2, Neininger et al 1996).

In those galaxies, where the CO emission falls faster than dust emission, the latter is correlated to the HI distribution (see also the case of NGC 1068, Papadopoulos & Seaquist 1999). This could be interpreted by two effects: there is an extended diffuse molecular component, not visible in the CO lines, because the H_2 density is not sufficient to excite the CO lines, or the CO abundance is depending non-linearly with metallicity, i.e. decreases more than the dust, which abundance is linear in Z . This might be the case in dwarf galaxies, as discussed in the next section.

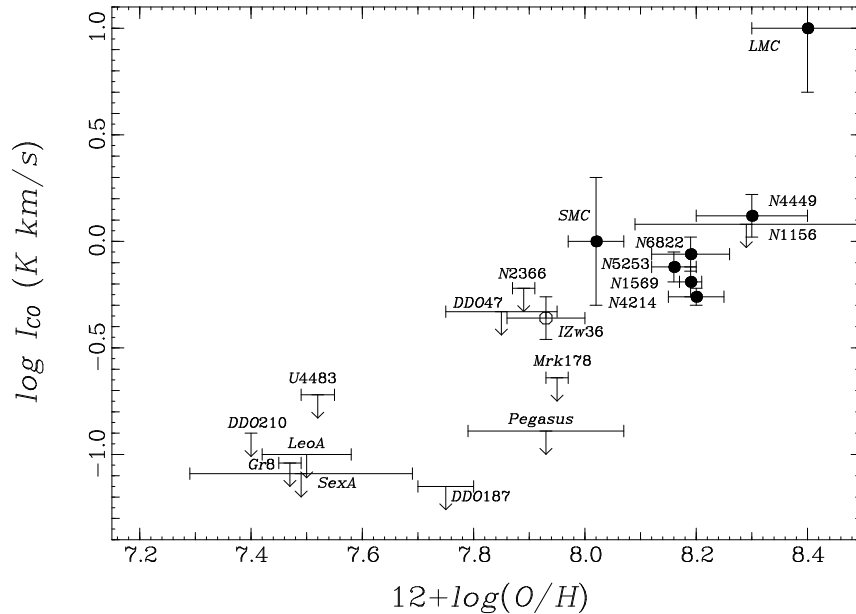


Figure 3. Dependence of the CO integrated intensity I_{CO} (normally proportional to the average H_2 surface density $N(H_2)$) on the oxygen abundance, or metallicity (from Taylor et al. 1998).

2. CO in dwarf galaxies and Blue Compact starbursts

Much effort has been devoted to the detection of CO lines in blue compact dwarf galaxies (BCDGs): their high star formation rates is assumed to require a large H_2 content, and its detection will help to understand the star formation mechanisms and efficiencies. But the task has revealed very difficult, since the objects have low masses, and low metallicity. Arnault et al. (1988) already suggested that X was varying as Z^{-1} , and even as Z^{-2} in a certain domain, but this was contested (Sage et al 1992). Recent results improve considerably the detection rate and the upper limits, because of the technical progress in the receivers (Barone et al 1998, Gondhalekar et al. 1998). They confirm the high dependence on metallicity of the CO emission.

Taylor et al. (1998) have tried to detect in CO HI-rich dwarf galaxies, in which the oxygen abundance was known. They have stringent upper limits on the most metal-poor galaxies, and conclude that the conversion factor must be varying nonlinearly with metallicity, increasing sharply below $\sim 1/10$ of the solar metallicity [$12 + \log(O/H) \leq 7.9$] (cf figure 3).

3. Low surface brightness galaxies: LSB

Low surface brightness galaxies may provide a clue to the galaxy evolution processes: they appear to be unevolved galaxies, with large gas fraction, which may have formed their stars only on the second half of the Hubble time (McGaugh

& de Blok 1997). Their metallicity is low, according to the correlation of metallicity with surface brightness (Vila-Costas & Edmunds 1992). Some can have however, very large masses (and large rotational velocities, implying large dark matter fractions). To tackle the mystery of their low-evolution rate, it is of prime importance to know their molecular content, and their total gas surface density. De Blok & van der Hulst (1998) have made a search for CO line emission in 3 late-type LSB galaxies: they find a clear CO-emission deficiency, and conclude to a molecular gas deficiency. They claim that the conversion factor X has not the same reasons to be higher than in normal late-type galaxies, since the star formation rate is smaller than in HSB galaxies, implying a lower UV flux, that does not photodissociate as much the CO molecules. However, their derived upper limits of the $M(\text{H}_2)/M(\text{HI})$ mass ratio fall in the same range as in HSB late-type galaxies; the question of their true molecular component is still open, the more so as early-type LSB galaxies are detected in CO. Note that there exists a large scatter of CO-emission or H_2 content, even in normal galaxies, and this is not well understood: in M81 for example, a particularly low H_2/HI interacting galaxy, with normal metallicity, the molecular clouds appear to have different characteristics, with a lower velocity dispersion at a given size (Brouillet et al. 1998).

Even with normal H_2/HI mass ratio (close to 1), the gas surface density of those LSB galaxies is lower than critical for gravitational instabilities, and that is sufficient to explain the low efficiency of star formation (van der Hulst et al. 1993, van Zee et al. 1997). These low surface densities could come from the poor environment and the lack of companions (Zaritsky & Lorrimer 1993).

4. Spiral Structure

It becomes now possible to map in the CO lines galaxies at large-scale, and with high spatial resolution, to have an overview of the molecular structure of a galaxy, with a high dynamical range. With the On-The-Fly mapping procedure, Neininger et al. (1998a) have surveyed nearly half of the M31 disk in CO(1-0) with $23''$ (90pc) resolution, and they have detailed some remarkable regions, at $2''$ resolution with the IRAM interferometer. Apart from emphasizing the fractal structure of the molecular gas over such large range of scales, this study reveals a tight correlation between the CO arms and the dust lanes, and also with the HI arms. At this scale, the kinematics of the CO lines are more dominated by the star forming shells and the resulting chaotic motions in the arms, than by large-scale streaming motions. In the global sense, the spiral structure of this galaxy is not well determined, due to projection effects, and it is possible that the ISM is concentrated more in a ring than in spiral arms (see the ISOPHOT map from Haas et al 1998).

The BIMA interferometer group has undertaken a survey of 44 nearby galaxies (SONG), with large fields of view (mosaics of 7 fields of $3-4'$), with $7''$ angular resolution (cf poster by Helfer et al., this conference). There is a large range of CO morphologies detected, among spirals, bars and rings. The spiral structure of M51 is particularly detailed, and the arm-interarm contrast deduced more exactly, including short-spacing.

5. Centers of galaxies

High-resolution CO maps of galaxy centers (at 100pc or less) have been obtained with interferometers. One of the striking features of the central H₂-component structure is the strong asymmetry observed, similar to what happens in the center of the Milky Way: the gas distribution is lopsided, and this appears to be the rule more than the exception.

One of the best example is the CO-rich M82 galaxy. Neininger et al (1998b) have recently performed a 4" resolution ¹³CO map with the IRAM interferometer. The map shows the same gross features as the ¹²CO one made by Shen & Lo (1995), i.e. a compact central source, and two offset maxima, that could be the signature of an edge-on ring. However, the central peak has a low ¹³CO/¹²CO ratio, may be due to a large UV-photodissociation (affecting selectively more the rarer isotopic species).

There is a strong velocity gradient in the CO, which is also a general rule in spiral galaxies (cf Sofue et al. 1997). The dynamical centre coincides with the IR peak and is shifted 6" north-east of the compact ¹³CO source, emphasizing the lopsidedness. The kinematics is also perturbed by star-formation shells, and around the most luminous compact radio source in M 82, is identified a 130 pc-wide bubble of molecular gas.

Another example is the edge-on warped galaxy NGC 5907, mapped in CO at 3" resolution by Garcia-Burillo et al. (1997). Spiral structure can be resolved in the center, which means that the galaxy is not completely edge-on (or strongly warped even in the molecular component). Non-circular motions are well explained by a bar rotating at a pattern speed of $\Omega_b = 70$ km/s/kpc (high enough to be that of a nuclear bar). The velocity gradient is high in the center, resulting from a massive and compact nuclear disk. This is interesting, since this galaxy could be classified as an early-type according to its nuclear velocity gradient, but has no bulge and is in fact classified as an Sc-Sd late-type. The molecular distribution is significantly off-centered and lopsided also in this galaxy.

6. Double bars and nuclear disks

Barred galaxies are conspicuous in general by their high concentrations of molecular gas in the center. They often possess nuclear disks, or large flattened gas concentrations in fast rotation, within the central 1kpc. This large molecular gas concentration can trigger starbursts, sometimes confined in nuclear rings (hot spots in H α).

The molecular distribution can have several morphologies, according to the presence of zero, one or two inner Lindblad resonances in the center. When there are Lindblad resonances, the gas accumulates in a spectacular twin-peaks morphology (Kenney 1996), corresponding to the crossing of the x1 orbits parallel to the bar, and the x2 orbits perpendicular to it, inside the ILR, generally materialised by a nuclear ring. This typical structure is nicely seen in NGC1530 mapped in CO by Reynaud & Downes (1997): the twin peaks are at the beginning of the characteristic thin dust lanes aligned with and leading the bar. In rare cases, there is only a single peak, may be due to the interaction with a companion (cf NGC5850, Leon et al 1999). When there is no ILR, in late-type

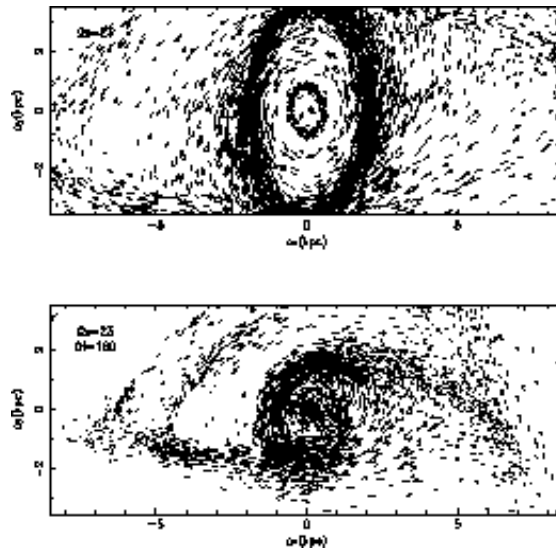


Figure 4. Particle orbits of molecular clouds in a simulation with only one pattern speed (top, $\Omega = 23$ km/s/kpc), and with two different pattern speeds for the two embedded bars (bottom, $\Omega = 23$ and 160 km/s/kpc), in M100, from Garcia-Burillo et al. (1998a). Only in the second case, a nuclear spiral structure is obtained, similar to the one observed in CO.

galaxies for instance, or when the pattern speed is relatively high, there is no ring, and only a central concentration (cf NGC 7479, Laine et al 1998).

Bars within bars is a frequently observed phenomenon, easy to see on color-color plots, or in NIR images of galaxies (to avoid dust extinction). The presence of an embedded bar has long been invoked as a mechanism to prolong the non-axisymmetry (and the resulting gravity torques) towards the center, to drive the gas and fuel an AGN (Shlosman et al 1989). Simulations have described the numerical process leading to the formation of double bars (Friedli & Martinet 1993, Combes 1994). In concentrating the mass towards the center, the first bar modifies the inner rotation curve, and the precessing rate ($\Omega - \kappa/2$) of the $m = 2$ elliptical orbits in the center increases to large values. This widens the region between the two ILRs, and mass accumulate on the perpendicular $x2$ orbits, which weakens the principal bar in this region. This strong differential $\Omega - \kappa/2$ prevents the self-gravity from matching all precessing rates in the center, and decoupling occurs: two bars rotating at two different pattern speeds develop. Eventually, a too large mass accumulation into the center can destroy the bar (Hasan et al 1993). To probe this scenario in double-bar galaxies, it is important to know the pattern speeds of the two bars, and derive the dynamical process at play.

A prototype of double-bar galaxies is NGC4321, or M100 (cf Knapen & Beckman 1996). The study of its molecular cloud distribution has been done at high resolution towards its central parts, including the nuclear bar (Sakamoto et al. 1995, Garcia-Burillo et al 1998a). A small nuclear spiral structure has

been detected inside the nuclear ring made of the star-forming hot spots. This morphology requires a model of nuclear bar with a very fast pattern speed ($\Omega = 160 \text{ km/s/kpc}$, see fig 4, from Garcia-Burillo et al. 1998a).

Sometimes, the gas in the center is also observed at high altitude above the plane (cf NGC 891, 5907, or N 4013, Garcia-Burillo et al. 1999). These might be accounted for by processes associated to the star-formation, more than purely dynamical mechanisms. The only exception could be gas in retrograde orbits.

Garcia-Burillo et al. (1998b) report for the first time the detection of a massive counterrotating molecular gas disk in the early-type spiral NGC3626. The CO emission is concentrated in a compact nuclear disk of average radius $r \sim 12''$ (1.2 kpc), rotating in a sense opposite to that of the stars, and in the same sense as the HII and HI gas (themselves counterrotating with respect to the stars). There is no evidence of a violent starburst in the center of the galaxy, which corresponds probably to the late stage of a merger.

7. Molecular content of cluster galaxies

Although many spiral galaxies in clusters are stripped from their HI gas, it has been established that they are not deficient in CO-emission, and probably also H₂ (Kenney & Young 1989 for Virgo; Boselli et al. 1995, Casoli et al. 1998 for Coma). This can be understood since the HI is usually located in the outer parts of galaxies, where the gas is less bound, and the tidal forces are larger; also the HI gas is more diffuse, and easier to deplete by ram pressure.

In Hickson compact groups, the molecular gas is not deficient either, and even enhanced in tidally interacting galaxies (Boselli et al. 1996, Leon et al. 1998, cf figure 5). In a particular Hickson group, the Stephan's Quintet, Xu & Tuffs (1998) have recently found evidence of a starburst going on outside galaxies. From ISOCAM $15 \mu\text{m}$ H α and NIR observations, they identified an outstanding bright source about 25kpc away from the neighbouring galaxies, containing very young stars, and corresponding to an SFR of about $0.7 M_{\odot}/\text{yr}$. They propose that the starburst is triggered by the collision between a fast galaxy and the IGM; alternatively this could be the formation of a tidal dwarf, through gravitational instabilities in a tidal tail (cf Duc & Mirabel 1998). Molecular gas (through CO emission) is difficult to detect so far from the nuclei (possibly because of metallicity gradients), and the detection in tidal tails are rare, like that in the NGC 2782 (Arp 215) tail by Smith et al. (1998).

8. Ultra-luminous IRAS galaxies

A new survey of ultra-luminous infrared galaxies with millimeter interferometer reveals that the molecular gas is confined in compact rotating nuclear disks or rings (Downes & Solomon 1998). The constraint that the gas mass is smaller than the dynamical mass imposes an excitation model in which the CO lines are only moderately optically thick ($\tau = 4 - 10$) and subthermally excited, so that the CO-to-H₂ conversion ratio is about 5 times less than standard. In that case, the fraction gas-to-dynamical mass is 15%. The surface density of gas, however, is in average $\mu_g/\mu_{tot} = 30\%$. In some cases, the CO position-velocity diagrams clearly shows a ring, with a central gap. In the particular case of Arp 220, there

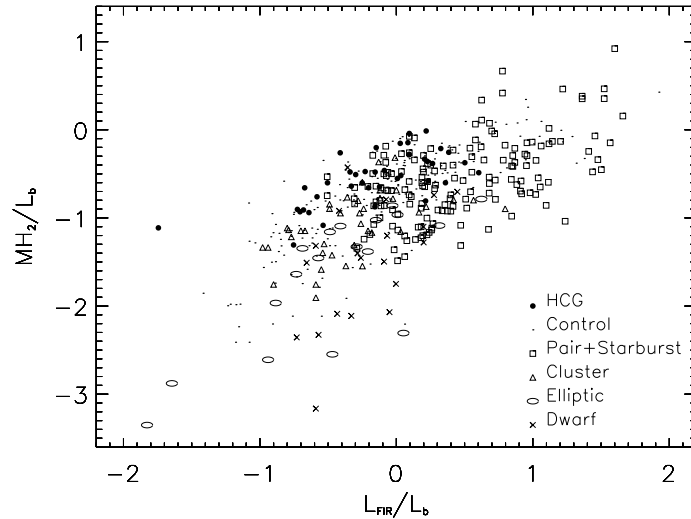


Figure 5. $M(\text{H}_2)$ versus $L(\text{FIR})$ normalised to Blue luminosity L_b for galaxies in compact groups HCG, compared to other samples (Control, Pairs and starbursts, Cluster, Elliptical and Dwarfs) from Leon et al. (1998).

appears to be two bright sources embedded in a central nuclear disk, which are compact extreme starburst regions, more likely than the premerger nuclei, as was previously thought.

An often debated question is whether the huge far infrared emission of the ultra-luminous galaxies are due to a starburst or a monster (AGN). It is frequent that both are present simultaneously, since they are both the results of huge mass accumulation in the centers of galaxies. Using ISO data, and diagnostic diagrams involving the ratio of high-to-low excitation mid-IR emission lines, together with the strength of the $7.7 \mu\text{m}$ “PAH” feature, Genzel et al. (1998) conclude that the far infrared emission appears to be powered predominantly by starbursts: 70%-80% are predominantly powered by recently formed massive stars, and 20%-30% are powered by a central AGN. Very high extinctions are measured towards these star-forming regions, supporting the high H_2 column densities derived from CO observations. In these objects, the active region is always sub-kpc in size.

9. Galaxies at high redshift

One of the most exciting results of these last years is the detection of galaxies at larger and larger redshifts, allowing to tackle the evolution and history of star formation in the Universe. After the first discovery in CO lines of an object at $z > 2$, the ultraluminous galaxy IRAS 10214+4724 (Brown & van den Bout

1992, Solomon et al 1992), there has been an extended search for more early starbursts, that resulted in the discovery of about 10 objects at high z in CO lines (cf Table 1).

Table 1. CO data for high redshift objects

| Source | z | CO line | S mJy | ΔV km/s | MH ₂ $10^{10} M_{\odot}$ | Ref |
|----------------|-------|------------|----------|--------------------|--|-----|
| F10214+4724 | 2.285 | 3-2 | 18 | 230 | 2* | 1 |
| 53W002 | 2.394 | 3-2 | 3 | 540 | 7 | 2 |
| H 1413+117 | 2.558 | 3-2 | 23 | 330 | 2-6 | 3 |
| SMM 14011+0252 | 2.565 | 3-2 | 13 | 200 | 5* | 4 |
| MG 0414+0534 | 2.639 | 3-2 | 4 | 580 | 5* | 5 |
| SMM 02399-0136 | 2.808 | 3-2 | 4 | 710 | 8* | 6 |
| APM 08279+5255 | 3.911 | 4-3 | 6 | 400 | 0.3* | 7 |
| BR 1335-0414 | 4.407 | 5-4 | 7 | 420 | 10 | 8 |
| BR 1202-0725 | 4.690 | 5-4 | 8 | 320 | 10 | 9 |

* corrected for magnification, when estimated

Masses have been rescaled to $H_0 = 75\text{km/s/Mpc}$. When multiple images are resolved, the flux corresponds to their sum

(1) Solomon et al. (1992a), Downes et al. (1995); (2) Scoville et al. (1997b); (3) Barvainis et al. (1994, 1997); (4) Frayer et al. (1999); (5) Barvainis et al. (1998); (6) Frayer et al. (1998); (7) Downes et al. (1998); (8) Guilloteau et al. (1997); (9) Omont et al. (1996a)

In fact the majority of these objects (if not all) are amplified by gravitational lenses, and this explains why they are detectable at all (see figure 6). The amplification is very helpful to detect these remote objects, but the drawbacks are significant uncertainties in the amplification factors, and therefore on the total molecular content. The excitation of the gas is also uncertain, since the various CO lines emission may have different spatial extents and different resulting amplifications.

One strategy to search for CO lines in high- z galaxies has been to select objects already detected in the far-infrared or submm dust emission. Indeed, all objects in Table 1 have been first detected in continuum, some (the SMM) have been discovered in blank field searches with the SCUBA bolometer on JCMT (Hawaii) by Smail et al. (1997). Since the emission of the dust is varying as ν^4 with the frequency ν in the millimeter range (until the maximum near $60\mu\text{m}$), it becomes easier to detect galaxies at $z = 5$ than $z = 1$ (cf Blain & Longair 1993). The millimeter domain is then a privileged one to follow the star-formation history as a function of redshift, and several surveys have been undertaken. Searches toward the Hubble Deep Field-North (Hughes et al 1998), and towards the Lockman hole and SSA13 (Barger et al 1998), have found a few sources, revealing an increase of starbursting galaxies with redshift. They correspond by extrapolation to a density of 800 per square degree, above 3 mJy at $850\mu\text{m}$. This already can account for 50% of the cosmic infra-red background (CIRB), that has been estimated by Puget et al (1996) and Hauser et al (1998)

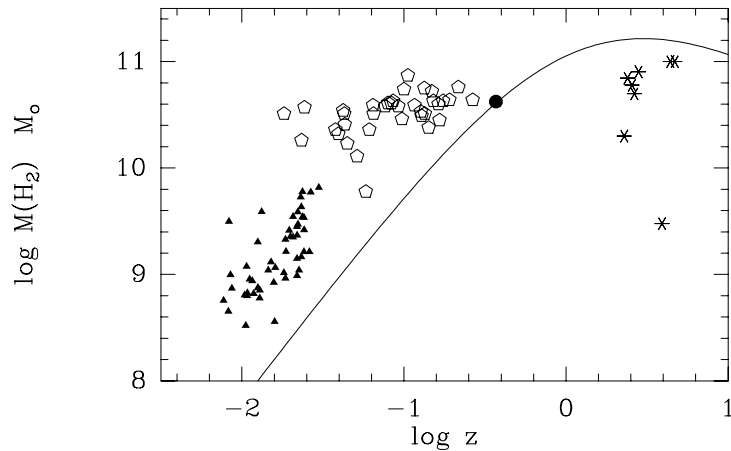


Figure 6. H_2 masses for the CO-detected objects at high redshift (filled stars), compared to the ultra-luminous-IR sample of Solomon et al (1997, open pentagons), and to the Coma supercluster sample from Casoli et al (1996, filled triangles). There is no detected object between 0.3 and 2.2 in redshift, except the quasar 3c48, marked as a filled dot (Scoville et al 1993, Wink et al 1997). The curve indicates the 3σ detection limit of $I(\text{CO}) = 1 \text{ K km/s}$ at the IRAM-30m telescope (equivalent to an rms of 1mK, with an assumed $\Delta V = 300\text{km/s}$). The points at high z can be detected well below this limit, since they are gravitationally amplified.

from COBE data. Similar conclusions have been reached towards the CFRS fields by Eales et al. (1999).

These first results show the potentiality of the millimeter domain, already with the present instruments. With the fore-coming next generation of mm telescopes, which will yield a factor 10-20 increase in sensitivity, it will be possible to detect not only huge starbursts but more ordinary galaxies at high redshift (cf Combes et al 1999).

References

- Arnault P., Kunth D., Casoli F., Combes F. 1988 *A&A* 205, 41
 Barger A.J., Cowie L.L., Sanders D.B. et al. 1998, *Nature* 394, 248
 Barone L.T., Heithausen A., Fritz T., Klein U. 1999, in *The Physics and Chemistry of the Interstellar Medium*, Proceedings of the 3rd Cologne-Zermatt Symposium, Zermatt, September 22-25, 1998, ed. V. Ossenkopf
 Barvainis R., Alloin D., Guilloteau S., Antonucci R. 1998, *ApJ* 492, L13
 Barvainis R., Tacconi L., Antonucci R., Coleman P. 1994, *Nature* 371, 586
 Blain A.W., Longair M.S. 1993, *MNRAS* 264, 509
 Boselli A., Casoli F., Lequeux J. 1995 *A&AS* 110, 521

- Boselli A., Mendes de Oliveira C., Balkowski C., Cayatte V., Casoli F. 1996 A&A 314, 738
- Brouillet N., Kaufman M., Combes F., Baudry A., Basch F. 1998 A&A 333, 92
- Brown R., Vanden Bout P. 1992, ApJ 397, L19
- Casoli F., Dickey J., Kazes I. et al. 1996, A&AS 116, 193
- Casoli F., Sauty S., Gerin M. et al. 1998, A&A 331, 451
- Combes F., Maoli R., Omont M. 1999, A&A in press
- Combes F. 1994, in Mass-transfer induced activity in galaxies, ed. I. Shlosman, Cambridge Univ. Press, p. 170
- de Blok W.J.G., van der Hulst J.M. 1998, A&A 336, 49
- Downes D., Neri R., Wiklind T., Wilner D.J., Shaver P. 1998, ApJ preprint (astro-ph/9810111)
- Downes D., Solomon P.M., Radford S.J.E. 1995, ApJ 453, L65
- Downes D., Solomon P.M. 1998 ApJ 507, 615
- Duc P.A., Mirabel I.F. 1998 A&A 333, 813
- Eales S.A., Lilly S.J., Gear W.K., Dunne L., Bond J.R., Hammer F., LeFevre O., Crampton D. 1999, ApJL in press (astro-ph/9808040)
- Frayser D.T., Ivison R.J., Scoville N.Z., et al., 1998, ApJ 506, L7
- Frayser D.T., Ivison R.J., Scoville N.Z., et al., 1999, ApJ preprint (astro-ph/9901311)
- Friedli D., Martinet L. 1993 A&A, 277, 27
- Garcia-Burillo S., Combes F., Neri R. 1999, A&A in press (astro-ph/9901068)
- Garcia-Burillo S., Sempere M.J., Combes F., Neri R. 1998a A&A, 333, 864
- Garcia-Burillo S., Sempere M.J., Bettoni D. 1998b ApJ 502, 235
- Garcia-Burillo S., Guelin M., Neininger N. 1997 A&A 319, 450
- Genzel R., Lutz D., Sturm E. et al. 1998 ApJ 498, 579
- Gondhalekar P.M., Johansson L.E.B., Brosch N., Glass I.S., Brinks E. 1998 A&A 335, 152
- Guelin M., Zylka R., Mezger P.G. et al. 1993, A&A 279, L37
- Guilloteau S., Omont A., McMahon R.G., Cox P., PetitJean P. 1997, A&A 328, L1
- Haas M., Lemke D., Stickel M. et al. 1998 A&A 338, L33
- Hasan H, Pfenniger D., Norman C. 1993 ApJ 409, 91
- Hauser M.G., Arendt R.G., Kelsall T., et al. 1998, ApJ 508, 25
- Hughes D.H., Serjeant S., Dunlop J. et al. 1998, Nature 394, 241
- Kenney J.D.P. 1996, in Barred galaxies, Astronomical Society of the Pacific Conference Series, Volume 91; edited by R. Buta, D. A. Crocker and B. G. Elmegreen, p.150
- Kenney J.D.P., Young J.S. 1989 ApJ 344, 171
- Knapen J.H., Beckman J.E. 1996, MNRAS 283, 251
- Laine S., Shlosman I., Heller C.H. 1998, MNRAS 297, 1052

- Leon S., Combes F., Friedli D. 1999, in "Galaxy Dynamics", Proceedings of Rutgers Conference, to appear in ASP Conf Series, ed. D. R. Merritt, M. Valuri, J.A. Sellwood
- Leon S., Combes F., Menon T.K. 1998 A&A 330, 37
- Maloney P., Black J.H. 1988, ApJ 325, 389
- McGaugh S., de Blok W.J.G 1997 ApJ 481, 689
- Neininger N., Guelin M., Ungerechts H. et al. 1998a, Nature 395, 871
- Neininger N., Guelin M., Klein U. et al. 1998b, A&A 339, 737
- Neininger N., Guelin M., Garcia-Burillo S. et al. 1996, A&A 310, 725
- Ohta K., Yamada T., Nakanishi K., Kohno K., Akiyama M., Kawabe R. 1996, Nature 382, 426
- Omont A., Petitjean P., Guilloteau S., McMahon R.G., Solomon P.M. 1996, Nature 382, 428
- Papadopoulos P.P., Seaquist E.R. 1999, ApJ preprint (astro-ph/9901346)
- Puget J.L., Abergel A., Bernard J-P. et al. 1996, A&A 308, L5
- Reynaud D., Downes D. 1997, A&A, 319, 737
- Rubio M., Lequeux J., Boulanger F. 1993, A&A 271, 9
- Ryder .D., Knapen J.H. 1999, MNRAS 302, L7
- Sage L.J., Salzer J.J., Loose H.H., Henkel C. 1992 A&A 265, 19
- Sakamoto K., Okumura S., Minezaki T. et al. 1995 AJ 110, 2075
- Scoville N.Z., Padin S., Sanders D.B. et al. 1993, ApJ 415, L75
- Scoville N.Z., Yun M.S., Windhorst R.A., Keel W.C., Armus L. 1997, ApJ 485, L21
- Shen J.J., Lo K.Y. 1995 ApJ, 445, L99
- Shlosman I., Frank J., Begelman M. 1989, Nature, 338, 45
- Smail I., Ivison R.J., Blain A.W. 1997, ApJL 490, L5
- Smith B.J., Struck C., Kenney J.D.P., Jogee S. 1998, AJ preprint (astro-ph/9811239)
- Sofue Y., Tutui Y., Honma M, Tomita A. 1997 AJ 114, 2428
- Solomon P.M., Downes D., Radford S.J.E., Barrett J.W. 1997, ApJ 478, 144
- Solomon P.M., Downes D., Radford S.J.E. 1992, Nature 356, 318
- Taylor C.L., Kobulnicky H.A., Skillman E.D. 1998, AJ 116, 2746
- van der Hulst J.M., Skillman E.D., Smith T.R. et al. 1993 AJ, 106, 548
- van Zee L., Haynes M.P., Salzer J.J. 1997 AJ 114, 2497
- Vila-Costas M.B., Edmunds M.G. 1992, MNRAS 259, 121
- Wilson C.D. 1995, ApJ 448, L97
- Wink J.E., Guilloteau S., Wilson T.L. 1997, A&A 322, 427
- Xu C., Tuffs R. 1998, ApJ preprint (astro-ph/9808344)
- Young, J., Knezek, M. 1989, ApJ, 347, L55
- Young, J., Scoville N.Z. 1991, A.R.A.A. 29, 581
- Zaritsky D., Lorrimer S.J. 1993 in The Evolution of Galaxies and Their Environment, Proceedings NASA. Ames Research Center, p. 82-83